Biochemistry (Moscow), Vol. 68, No. 6, 2003, pp. 662-677. Translated from Biokhimiya, Vol. 68, No. 6, 2003, pp. 810-827.

Structural–Functional Organization of the Main Light Harvesting Complex and Photosystem 2 of Higher Plants

V. L. Tetenkin

Department of Biophysics, School of Biology, Lomonosov Moscow State University, Moscow 119992, Russia; fax: (095) 939-1115; E-mail: teten3@okclub.org

Received February 4, 2002
Revision received April 12, 2002

Abstract—The interrelation between spectral and structural–functional properties of LhcIIb was studied. The dipole strength of the main Q_y bands of chlorophylls (Chl *a* 30.8 D^2; Chl *b* 18.5 D^2) and chlorophyll *a/b* ratio (Chl *a*/Chl *b* = 7 : 6) were determined for LhcIIb. The Chl *a*/Chl *b* value shows that the subunit of this complex contains seven Chl *a* and six Chl *b* molecules. Individual bands of chlorophylls (bands in stokes and anti-Stokes parts at 77 K were Lorentzian and Gaussian, respectively) were resolved using synchronized deconvolution of absorption, CD, and LD bands of chlorophylls. Seven of these bands belonged to Chl *a*. Parameters of absorption bands of Chl *a* indicate that seven molecules represent a united cluster (heptamer) with exciton interactions, determining the spectrum of LhcIIb in the Chl *a* absorption region. Parameters of absorption bands of Chl *b* show the existence of three clusters: monomer (639.6 nm), dimer (645.2 and 647.4 nm), and trimer (649.8 and 654.1 nm). These clusters and their properties agree with the well-known structure of porphyrin groups of the LhcIIb subunit (Kuhlbrandt, 1994). A distorted ring of seven porphyrins in the stromal range of the subunit corresponds to Chl *a* heptamer; a separately located molecule near the N-terminal domain on the stromal side of the subunit corresponds to Chl *b* monomer; a dimer and a trimer of porphyrins in the lumenal range of the subunit correspond to the dimer and trimer of Chl *b*, respectively. The calculated lifetimes of the excitation energy (exciton) transfer in subunit and trimer of LhcIIb confirm this location of pigments. The geometry of the Chl *a* heptamer (mutual orientation of transition dipole moments) was determined by the steady-state Kasha–Tinoco approximation using parameters of individual bands of exciton splitting. The calculated parameters of mutual orientation of Chl *a* dipoles agree with the topography of the stromal porphyrins found by electron crystallography (Kuhlbrandt, 1994). A structural model of the granal multicentral macrocomplex of PSII (*M*PSII) is suggested. The lifetimes of the exciton migration between the main pigment–protein compartments of *M*PSII were calculated. The results of calculation are consistent with the structural model of the photosystem. The location of pigments provides for fast exciton hopping between Chl *a* clusters of neighboring proteins in the *M*PSII along the stromal surface within the membrane (5-25 psec) and between stacked membranes (~40 psec) of chloroplast grana.

Key words: photosynthesis, light-harvesting complex, LhcII, pigment–protein complex, antenna, spectroscopy, energy migration, exciton, Photosystem 2, PSII

Virtually the whole pigment apparatus of photosynthesis is involved in the processes of absorption of photons and migration of excitation energy (exciton) by radiationless transfer between pigment molecules (excitation energy migration) to photosynthetic reaction centers, which contain only a minor fraction of chlorophyll [1] and mediate exciton dissociation and primary stabilization of separated charges (an electron at the acceptor side and a hole at the donor side of the RC).

The main light-harvesting complex of higher plants contains most of the chlorophyll and a significant fraction of protein of the granal region of the chloroplast. This complex plays a decisive role in formation and stabilization of the photosynthetic supramolecular membrane structures and balanced energy supply to reaction centers of Photosystems 1 and 2. The main light-harvesting pigment–protein trimer complex of higher plants (LhcIIb)

Abbreviations: Lhc) chlorophyll *b*-containing light-harvesting pigment–protein complex; LhcIIb) main light-harvesting pigment–protein trimer complex of higher plants; CON) minor Lhc connecting LhcIIb and PSII; PPC) pigment–protein complex; PSII) Photosystem 2; OD) optical density (absorbance); CD) circular dichroism or absorption difference between light beams with left and right circular polarization; LD) linear dichroism or absorption difference between light beams with parallel and perpendicular linear polarization; F) fluorescence; Chl *a*) chlorophyll *a*; Chl *b*) chlorophyll *b*; *Car*) carotenoid(s) incorporated in LhcIIb (lutein); RC) photosynthetic reaction center; *M*PSII) multicentral (granal) macrocomplex of Photosystem 2.

0006-2979/03/6806-0662$25.00 ©2003 MAIK "Nauka/Interperiodica"

and its aggregates[1] have been studied in our laboratory for more than 20 years [2-5]. For the first time we succeeded in isolating this complex in a state close to native and studied the fine structure of its spectra. The LhcIIb apoprotein is a functional container for chlorophyll molecules: internal structure of the protein provides binding of a large number of chlorophyll molecules and their stabilization, preventing thereby formation of non-fluorescent aggregates of chlorophyll. The surface properties of the complex provide necessary spatial localization of protein, interaction with photoactive complexes, and effective transfer of excitation energy to the RC.

The three-dimensional structure of LhcIIb was resolved by Kuhlbrandt et al. using electron crystallography with spatial resolution of 6 Å [6] and 3.4 Å [7] and localization of 12-13 porphyrin molecules in the LhcIIb subunit. The Chl *a*/Chl *b* ratio in the LhcIIb preparations studied in [6] and [7] was determined to be 1.1 and 1.33, respectively. This discrepancy was due to the difference between the methods of measurement of chlorophyll concentration used in these works. It should be noted that neither of the two values of this ratio fits the crystallographic data reported in these works. In my opinion, the pattern of distribution of chlorophyll molecules over the binding sites in the subunit suggested in [7] is not very convincing because it is based *exclusively* on the efficiency of quenching of triplet states. According to this logic, it is impossible to identify the chlorophyll-13 molecule located separately near the N-terminal domain of the subunit. Perhaps, this was the reason for not showing this molecule in the structural diagram suggested in [7].

The whole family of the Lhc proteins has now been sequenced. It was found that these proteins are characterized by a high degree of homology [8], and their concentrations in chloroplasts have been determined [8, 9]. This family includes ten different proteins. Three of ten have very similar composition, constitute the most part of bulk protein, and form LhcIIb, whereas the other seven proteins connect LhcIIb with Photosystems 1 and 2 [8, 9].

Spectra of OD, CD, LD, F, and polarization of F [2, 3, 10-12] and dynamics of OD changes within a broad time range [10, 11, 13-15] have been studied. It was shown that spectral properties of LhcIIb and isolated subunit of LhcIIb coincide with one another within the Chl *a* range [16, 17], whereas minor discrepancy between the spectral properties of the subunit and trimer within the Chl *b* range [16, 17] can be explained by the conformational changes of the LhcIIb subunit during trimer dissociation. The characteristic time of the excitation energy transfer between pigment molecules ($\sim 10^{-13}$ sec) was measured [11, 13, 15], and a thermal equilibrium between populations of electron transitions in LhcIIb was demonstrated [14, 18, 19]. Dense packing of chlorophyll molecules in LhcIIb [7] necessarily gives rise to the exciton interaction between pigment molecules and formation of exciton[1] and exciton splitting [5, 20]. The exciton splitting itself gives rise to fine structurization of the OD and LD spectra, alternation-sign and conservative CD, and thermally equilibrated fluorescence.

Results obtained in our laboratory demonstrated that the steady-state absorption (OD, LD, and CD) spectra were determined by concentration and structure of the exciton clusters of chlorophyll in the protein subunit of interest. The exciton dynamics (excitation energy migration) was determined by mutual orientation of these clusters and it was manifested in the steady-state spectra of fluorescence [5, 21, 22]. The whole aggregate of the primary processes of photosynthesis can be quantitatively described in terms of exciton structure and exciton dynamics. The most important structural and kinetic parameters of these processes can be calculated from the steady-state spectra of the pigment–protein complexes (PPC), photosystems, and chloroplast membranes.

The goal of this work was to study correlation between spectral, structural, and functional properties of LhcIIb. In spite of a large number of mathematical formulas used in this work, the sense of the results obtained is fairly simple and illustrative. A uniform component of LhcIIb corresponding to the native form of LhcIIb was found. The number of chlorophyll molecules in this complex was determined, and parameters of individual spectral bands of chlorophyll were calculated. The use of these parameters within the framework of the exciton theory allowed the mutual location of pigments within the LhcIIb subunit as well as the interaction between the pigments to be calculated. The spatiotemporal characteristics of the processes of excitation energy migration between subunits in the granal macrocomplexes *M*PSII of chloroplasts were estimated and their functional analysis was performed.

MATERIALS AND METHODS

Cells of the cyanobacterium *Anacystis nidulans* R2 were grown in Kratz–Meyers liquid medium as described earlier [21]. Cells of chlorella (*Chlorella vulgaris* Beijer, thermophylic strain S-39/64688) were a gift of L. V. Shenderova. Cells were grown at 30°C and light intensity 30 W/m^2.

To isolate membranes, cells of cyanobacteria and chlorella were ground together with corundum powder (1 min in 50 mM Tris-HCl buffer, pH 7.0) in a thin layer of a dense suspension of cells on a glass plate cooled to 4°C using a ground Petri dish. Photosynthetic membranes were isolated from the homogenate by differential centrifugation as described earlier [21]. Membranes *M*PSII

[1] The nomenclature of light-harvesting complexes (Lhc) suggested by Peter and Thornber [9] is used.

[1] Exciton is a collective excited state of closely located pigments. Exciton cluster is an isolated ensemble of molecules, excitation of which gives rise to exciton formation.

were isolated from chloroplasts of two-week-old seedlings of pea (*Pisum sativum* L.). Aggregated forms of LhcIIb were isolated from membranes *M*PSII as described elsewhere [2, 4]. Spectra of aggregated forms of LhcII were measured in the presence of 0.02% Triton X-100.

Oligomeric forms of LhcII, including LhcIIb, were isolated electrophoretically from the fraction of the *M*PSII membranes obtained during isolation of aggregated LhcIIb. Gel electrophoresis of membranes solubilized in 1% Triton X-100 was performed in the cold in 7.5% polyacrylamide gel and 50 mM Tris-glycine buffer (pH 8.3) containing 0.01% sodium dodecyl sulfate as described earlier [21]. Electrophoresis was run simultaneously in several glass tubes (diameter, ~1 cm). Stained zones containing PPC were cut from the gel columns and their spectral properties were studied in gel tablets *in situ*. The preparations of corresponding zones obtained in parallel during the same electrophoretic run were considered as duplicate, triplicate, etc. measurements of the same sample. If necessary, the preparations were stored in the dark and in the cold in Tris-HCl buffer.

The absolute quantum yield of fluorescence of aggregated LhcIIb was measured as described in [22] using fluorescence of free chlorophyll as an internal standard.

Spectra of OD and LD were measured using an SF-14M spectrophotometer equipped with an integrating sphere, a low-temperature unit, and a dichroic unit. To measure absorption spectra at 77 K, gel tablets with samples were soaked in 70% glycerol for 1 h under continuous stirring in the cold. To measure LD spectra, a gel tablet soaked in glycerol was stretched and frozen above liquid nitrogen. LD spectrum was recorded as the absorption difference between light beams with parallel and perpendicular linear polarization relative to the axis of gel stretching ($A_{\parallel} - A_{\perp}$).

Spectra of fluorescence and fluorescence excitation were measured using a SPIL TsKB AN SSSR spectrofluorometer. Spectra were corrected for spectral sensitivity of photodetector and spectral distribution of light source. CD spectra were measured using a Jasco-40 AS dichrograph. All spectra were corrected for the baseline shape.

Concentrations of chlorophylls were determined spectrophotometrically in 80% aqueous acetone using the Vernon equation [23] modified for molar concentrations:

$$C\,(\mu\mathrm{M}) = \left\{ \begin{array}{l} -2.67\ D_{649} + 13.02\ D_{665}\ (\mathrm{Chl}\ a) \\ +22.16\ D_{649} - 5.71\ D_{665}\ (\mathrm{Chl}\ b) \end{array} \right\}; \qquad (1)$$

where D_{649}, D_{665} are the optical densities of the extracts at 649 and 665 nm, respectively.

The dipole strength and rotation strength ($D \times M$ = Debye × Bohr magneton) of the electronic transitions were calculated using equations derived from the following standard formulas [24]:

$$\mu^2\,(\mathrm{D}^2) = 9.18 \cdot 10^{-3}\,\lambda_0^{-1} \int \varepsilon(\lambda)\mathrm{d}\lambda\ ; \qquad (2)$$

$$C\,(\mathrm{D} \times \mathrm{M}) = 3.00 \cdot 10^{-2}\,\lambda_0^{-1} \int \theta(\lambda)\mathrm{d}\lambda\ ; \qquad (3)$$

where λ_0 is the wavelength of the spectral maximum (nm), μ is the dipole moment of the transition (D), $\varepsilon(\lambda)$ is the spectrum of the molar extinction coefficient ($\mathrm{M}^{-1}\cdot\mathrm{cm}^{-1}$), $\theta(\lambda)$ is the spectrum of the molar ellipticity ($\mathrm{deg}\cdot\mathrm{M}^{-1}\cdot\mathrm{cm}^{-1}$).

The rate constants of fluorescence and inductive resonance migration (Förster) were calculated using equations derived from the following standard formulas [24, 25]:

$$k_f\,(\mathrm{sec}^{-1}) = \tau_0^{-1} = 2.89 \cdot 10^{-9} \cdot n^2 \int \nu^{-1} F(\nu)\mathrm{d}\nu; \qquad (4)$$

$$k_m\,(\mathrm{sec}^{-1}) = 2.54 \cdot 10^{9} \cdot k^2 \cdot n^{-2} \cdot R^{-6} \int \nu^{-5} F(\nu) \times \varepsilon(\nu)\mathrm{d}\nu; \qquad (5)$$

where $\varepsilon(\nu)$ is the spectrum of the molar extinction coefficient of the acceptor; $F(\nu)$ is the power spectrum of the donor fluoresce; ν is the wavenumber (cm^{-1}); τ_0 is the natural lifetime of the excitation donor (sec); R is the distance between the dipoles (nm); n is the refraction index of the medium; $k = \cos(\alpha) - 3\cos(\beta)\cos(\gamma)$ is the orientation factor; α is the angle between the dipole moments of transitions; β and γ are the angles between the dipole moments of transitions and the radius-vector connecting the dipoles; $0 \le k^2 \le 4$, the mean three-dimensional value of $k^2 = 2/3$; the mean two-dimensional value on a plane, $k^2 = 5/4$. These equations allow the integration to be performed within a narrow frequency band and they are valid for elaborate spectra, provided the condition of thermal equilibrium is observed, i.e., the universal Stepanov equation is valid [26]:

$$F(\nu) = \varepsilon(\nu) \cdot \nu^3 \exp\left(\frac{\nu_0 - \nu}{kT}\right); \qquad (6)$$

where ν_0 is the energy of the 0–0 transition; the ratio of the rate constants or direct and back reactions of energy migration in this case is equal to the ratio of corresponding integrals in Eq. (5).

The angles between the normal to the LhcIIb plane and the dipole moment of the transition were calculated from the equation for the LD anisotropy:

$$\overline{\mathrm{LD}}_i = \Delta A_i / A_i = Const \cdot [1 - 3\cos^2(\alpha_i)]; \qquad (7)$$

where $\overline{\mathrm{LD}}_i$ is the linear dichroism anisotropy of the i-th transition; A_i is the isotropic absorption (optical density) of the i-th transition; $\Delta A_i = (A_{\parallel} - A_{\perp})_i$ is the linear dichroism of the i-th transition; α_i is the angle between $\overline{\mu}_i$ and the normal to the plane of the LhcIIb structure; *Const* is determined by the anisotropy of the medium (method of orientation and degree of ordering) and ranges from 0 to 1 during transition from disordered system to ideal order.

The energy, dipole strength, and rotation strength of CD for the resonance exciton interaction between the transition dipole moments $\overline{\mu_i}$ and $\overline{\mu_k}$ were calculated using the steady-state Kasha–Tinoco approximation for point dipoles [24, 27]:

$$E_{ik}\ (cm^{-1}) = 5.04\ \mu_0^2\ k\ R^{-3};$$

$$m_{ik} = \mu_0^2 [1 \pm \cos(\alpha)]; \quad (8)$$

$$c_{ik} = \frac{340}{\lambda_0} (\overline{\mu_i} \times \overline{\mu_k}) \cdot \overline{R_{ik}};$$

where $\overline{R_{ik}}$ is the radius-vector between the dipole centers (nm); symbol × denotes vector multiplication; k and R (nm) are the orientation factor and distance, respectively; μ_0^2 is the dipole strength of the monomer transition (D^2).

Bands of elaborate shape were used to resolve the spectra into individual spectral bands. Vibrational bands were described by symmetric curves of normal Gaussian distribution; the Stokes arm of the main bands was described by Lorentzian distribution; the anti-Stokes arm of the bands at 77 K was described by Gaussian distribution; the anti-Stokes arm of the bands at room temperature was described by a curve of the lag-distribution (intermediate between Lorentzian and Gaussian):

$$A(\Delta) = \frac{A_0}{[ch(\Delta)]^2};$$

$$\Delta = \frac{(\lambda - \lambda_0)\ln(3 + \sqrt{8})}{2b}; \quad (9)$$

where λ_0 is the wavelength (nm) of the spectral maximum A_0; ch is the hyperbolic cosine; b is the half-width of the band (nm) (width at half-height). Band asymmetry (ratio of half-width parameters of Stokes and anti-Stokes arms) was used to characterize the shape of the spectral bands.

Spectral data were processed and all calculations were performed using the MATLAB computer programs (Math Works, USA).

RESULTS AND DISCUSSION

Pigment composition of LhcIIb. Spectral parameters and concentration of chlorophylls in the LhcIIb subunit were studied in acetone extracts of six different samples of LhcII, the concentration of chlorophyll in which was determined from Eq. (1), and extract of membranes of the cyanobacterium *A. nidulans* containing no Chl *b*. The digital (discrete) spectrum of the *i*-th sample can be represented as a numerical vector $A_i = f_i(\lambda_k)$, whereas the aggregate of the seven spectra of the tested extracts can be represented as the matrix $\boldsymbol{A} = \{A_i\}$; concentration $\boldsymbol{C}$ = {Chl *a*, Chl *b*} was determined as the matrix of two spectra of chlorophylls *a* and *b* in the optical density units ($mM^{-1}\cdot cm^{-1}$); $\boldsymbol{K} = \{K_i\}$ is the matrix of concentrations of chlorophylls in the extracts. By definition, $A_i = C\cdot K_i$, or for all spectra $\mathbf{A} = \mathbf{C}\cdot\mathbf{K}$. Spectra of chlorophylls were calculated using the inverse regression equation $\boldsymbol{C} = \boldsymbol{A}\cdot\boldsymbol{K}'(\boldsymbol{K}\cdot\boldsymbol{K}')^{-1}$, where the symbol ′ denotes transposition. The spectra calculated using these equations are shown in Fig. 1a. Parameters of chlorophyll bands were determined by resolving spectra into individual bands. Integration of Eq. (2) allows the dipole strength of pigments to be determined: μ_0^2 (the main Q_y-band of Chl *a*) = 30.8 D^2; μ_0^2 (the main Q_y-band of Chl *b*) = 18.5 D^2.

Spectral analysis allowed the formulas for describing the shape of individual bands to be derived (see "Materials and Methods"). The Lorentzian shape of the Stokes slope in OD spectra is masked by short-wavelength transitions. However, this shape is clearly seen in the long-wavelength slope of the F spectrum (Fig. 1b).

Substitution of Chl *a* parameters (τ_0 = 15.2 nsec [24]) into Eq. (4) gives n = 1.35, which coincides with the standard value of the refraction index of acetone. The shape of the spectra, positions of spectral maximums, and values of extinction coefficients of chlorophylls coincided with similar data reported by Vernon [23]. The shape of the Chl *b* spectrum was realistic and close to the shape of the Chl *a* spectrum, whereas the Chl *a* spectrum coincided with the spectrum of the cyanobacterial extract. These results show that the method of Vernon is good for determining chlorophyll concentration.

The Chl *a*/Chl *b* ratio in LhcIIb preparations was calculated using Eq. (1) as Chl *a*/Chl *b* = 1.17 = 7 : 6. This value is consistent with the crystallographic data: the LhcIIb subunit contains 12-13 molecules of chlorophyll [7] and it can be suggested that the LhcIIb subunit contains seven molecules of Chl *a* and six molecules of Chl *b*.

Component composition of LhcII. Statistical processing of OD spectra of various LhcII preparations revealed four spectral components, superposition of which gives rise to spectral difference between LhcII preparations. Components 1-3 are characterized by the same Chl *a*/Chl *b* ratio and their spectra are variants of the LhcIIb spectrum. Component 3 is formed during aging or heating of samples. Component 2 is typical of certain spectra of LhcIIb aggregates. Spectral parameters, structure, and pigment composition of component 1 correspond those in native LhcIIb [5]. Component 4 (molar ratio component 4/component 1 = 1 : 3) is observed in the electrophoretic zone of the molecular weight of the LhcII tetramer and corresponds to a CON-protein [9]. As a minor admixture, component 4 is observed in preparations of aggregated LhcIIb. Absorption spectra of these complexes and a diagram of their origin are shown in Fig. 2.

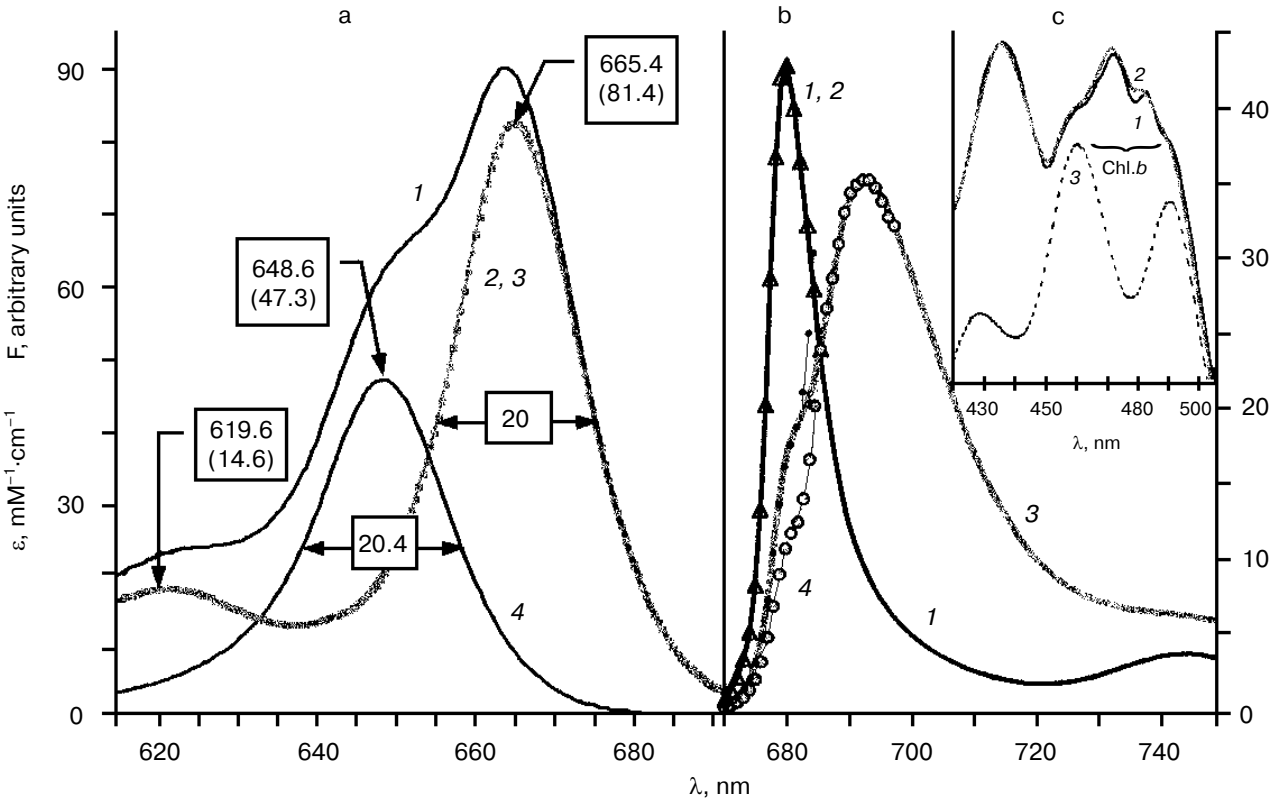

Fig. 1. Spectra of LhcIIb and its pigment extracts. a) Absorption spectra in 80% acetone at room temperature (left scale): *1*) spectrum of LhcIIb extract; *2*) (dotted line) spectrum of *A. nidulans* extract; *3*) calculated spectrum of Chl *a*; *4*) calculated spectrum of Chl *b*. The wavelength of spectral maximums, millimolar extinction coefficients, and spectral band half-width values are shown. b) Fluorescence (F) spectra of two LhcIIb samples. Spectra were normalized to area; *1*) freshly prepared preparation = component 1 (left scale); *3*) preparation after one-week storage = component 3 (right scale). Dotted lines (*2*, *4*) show the F spectra calculated from the OD spectra of the preparations using the Stepanov equation. c) Spectra of carotenoid and LhcIIb extracts in blue-green spectral range at 77 K (right scale): *1*, *2*) spectra of LhcIIb; *3*) absorption spectrum of carotenoid extract in 1% Triton X-100. *1*) OD; *2*) fluorescence excitation spectrum (detection λ, 682 nm); Chl *b*) Soret band of Chl *b*.

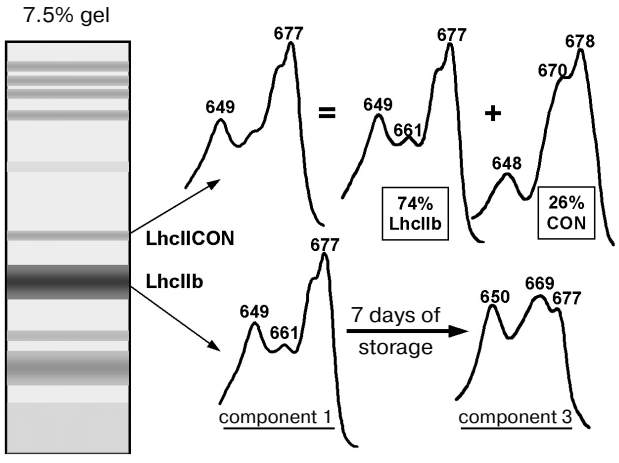

Fig. 2. Diagram of a polyacrylamide gel column after electrophoresis of *M*PSII membranes and absorption spectra of electrophoretic bands of LhcIIb trimer and tetramer.

Fluorescence spectra of two LhcIIb preparations corresponding to component 1 (freshly prepared preparation of LhcIIb trimer) and component 3 (old preparation stored for one week) are shown in Fig. 1b. The fluorescence spectrum of the fresh preparation calculated from its absorption spectrum using Eq. (6) is shown in Fig. 1b, curve *2*. This spectrum coincides with the experimentally measured spectrum of F (Fig. 1b, curve *1*). This coincidence indicates high efficiency of the excitation energy migration in this sample, implying thereby its nativeness and homogeneity. This suggestion is also confirmed by the long fluorescence lifetime of this preparation (~2 nsec at room temperature, which was much longer than in other PPC) and sharply resolved structure of absorption spectra at 77 K. High efficiency of excitation energy migration between pigments in this sample is supported by the coincidence of the fluorescence excitation spectrum with the absorption spectrum (Fig. 1c).

Aging of LhcIIb preparations is accompanied by disappearance of typical fine structure of the OD spectra and appearance of broad absorption bands in the short-wavelength (maximum at 668-669 nm) and long-wavelength (maximum at about 680 nm) spectral ranges. Repeat electrophoresis revealed that although the trimer structure was conserved in old samples, the general shape of the OD spectrum of old LhcIIb (Fig. 2) was close to the LhcII spectrum of chlorella. These data suggest that the aging-induced deformation of LhcIIb is a conformational transition rather than trivial denaturation of protein.

The amplitude of the long-wavelength absorption band gradually increases upon aging the LhcIIb, whereas the amplitude of the LhcIIb fluorescence band depends on the fraction of deformed LhcIIb and on the degree of LhcIIb aggregation. The higher is the contribution of this band to the overall fluorescence, the lower is the quantum yield of F (the shorter is the fluorescence lifetime): the quantum yield of fluorescence of old LhcIIb preparation is decreased to approximately one-tenth of the quantum yield of fluorescence of fresh preparation. It should also be noted that excitation quenching in antenna exerts an unfavorable effect on the efficiency of excitation transition to reaction centers. If such quenching existed *in vivo*, it would be functionally important for limiting the amount of light quanta migrating to the RC.

Spectral properties of LhcIIb. It was noted above that statistical processing of spectral data revealed a structurally uniform sample consisted of virtually pure and native LhcIIb, certain spectra of which are shown in Fig. 1. To attain this goal, the OD, CD, and LD spectra shown in Fig. 3a were used. The parameters of synchronous deconvolution of corresponding spectra are given in Table 1.

The long-wavelength band near 680 nm corresponding to parameters of band 1 (Table 1) was observed in LhcIIb using the hole burning method at 4 K [15].

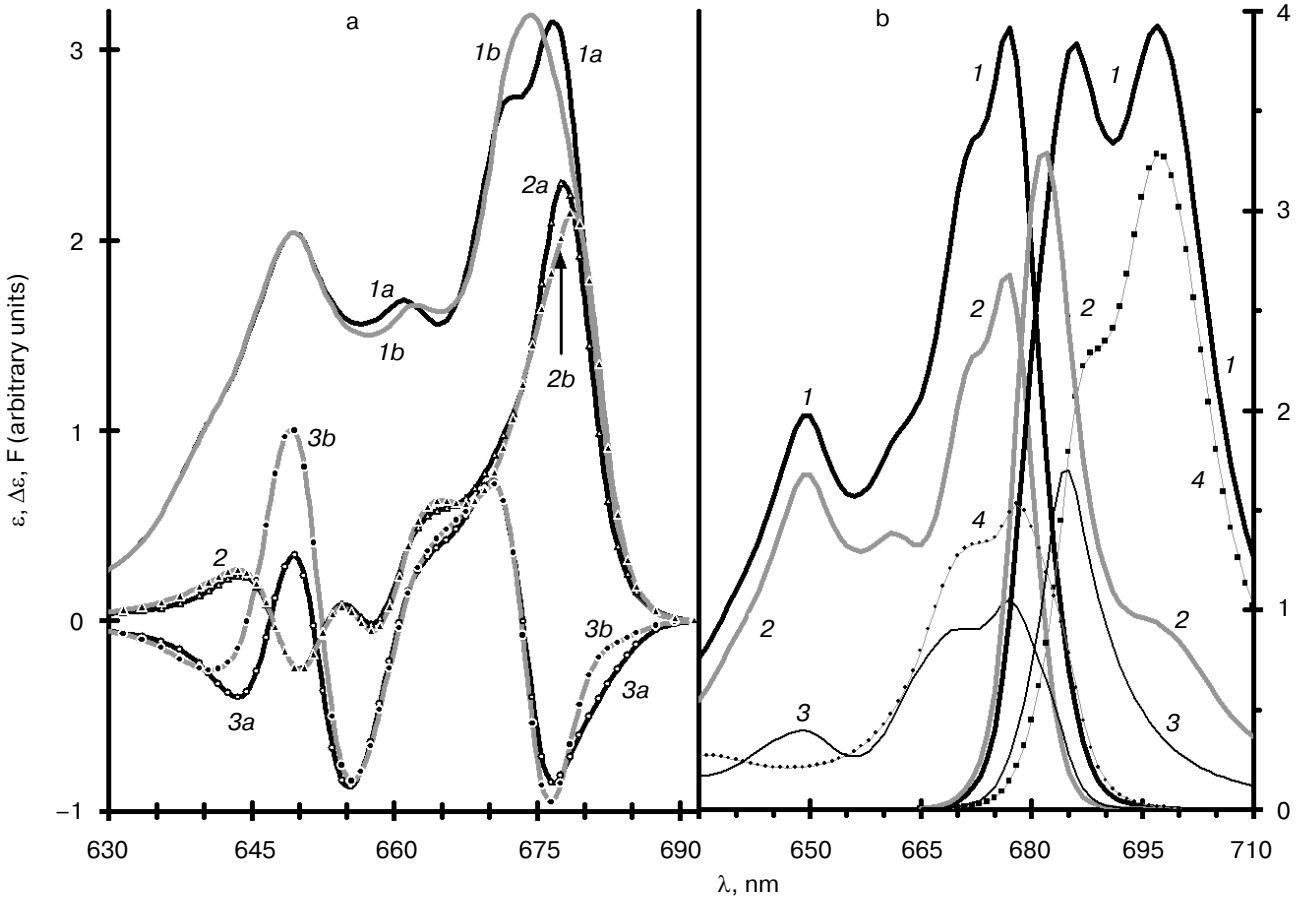

Fig. 3. Spectra of LhcIIb, photosynthetic membranes, and *M*PSII components at 77 K. a) Absorption-type spectra of LhcIIb: *1*) OD; *2*) LD; *3*) CD; indices *a* and *b* correspond to experimentally measured and calculated for exciton clusters, respectively (spectral parameters are given in Table 1). Spectra are shown without vibrational bands. b) Spectra of *M*PSII membranes and their components (arbitrary units): *1*) *M*PSII membranes; *2*) LhcIIb isolated from *M*PSII (fluorescence ×2, i.e., extended twofold); *3*) CON (absorption ×2); *4*) (dashed line) core-complex (absorption ×2). Spectrum No. 1 (OD or F) is a weighted sum of spectra Nos. 2, 3, and 4 (No. 1 = Σ(2 + 3 + 4)) with scaling factors.

Table 1. Parameters of absorption spectra of LhcIIb at 77 K. Parameters of exciton spectra derived from structural models using the Kasha–Tinoco theory are indicated italic. Model parameters are given in Table 2. Spectra are shown in Fig. 3a

No.	Vibrational		Chlorophyll *b*					Chlorophyll *a*						
			B1	*B2*		*B3*		*A7*						
	14	13	12	11	10	9	8	7	6	5	4	3	2	1
λ (nm)	618.7 618.7	631.0 631.0	639.6 639.6	645.2 *645.2*	647.4 *647.4*	649.8 *649.8*	654.1 *654.1*	658.1 *658.1*	661.5 *662.1*	667.2 *666.7*	671.0 *671.5*	676.4 *675.5*	678.0 *679.1*	680.8 *680.4*
Δλ (nm)	15.6	15.8	9.7	9.1	7.7	6.6	7.8	7.9	8.5	5.8	7.0	7.3	6.1	8.5
Asymmetry	1	1	1.15	1.30	1.04	1.24	1.00	1.17	1.04	1.29	1.27	1.03	1.17	1.03
μ^2 (D^2)	29.1	10.6	18.7 *18.5*	21.0 *21.4*	15.2 *15.6*	27.7 *27.6*	28.3 *27.9*	11.7 *12.5*	38.3 *37.9*	6.3 *5.6*	56.0 *54.2*	65.2 *67.2*	28.5 *26.0*	9.8 *12.1*
CD (D × M)	0.4	0.5	0.3 *0*	−11.6 *−10.0*	5.7 *10.0*	7.3 *10.9*	−10.9 *−10.9*	−3.8 *−4.0*	3.8 *3.8*	0.7 *1.2*	10.8 *12.7*	−12.6 *−13.7*	3.7 *2.3*	−3.4 *−2.3*
$\overline{LD}$	0.0	0.1	0.0	0.6 *0.6*	−0.2 *−0.2*	−0.3 *−0.3*	0.2 *0.2*	−1.2 *−1.1*	0.3 *0.4*	0.2 *0.2*	0.1 *0.1*	0.2 *0.3*	1 *1.0*	0.8 *0.8*
∠α (°)	55	57	54	68	51	48	60	31	62	59	58	59	90	77
$\frac{\Sigma\mu_i^2}{\mu_0^2}$	Number of molecules* per subunit													
	—	—	1.0	2.0		3.0		7.0						

* Ratio of the sum of the dipole strengths of the spectral bands to the dipole strength of absorption of corresponding pigment monomer (basis of isolation of a cluster).

The angles given in Table 1 were calculated from Eq. (7), the value of *Const* in which was calculated by substituting the maximum value ∠α = 90° for band 2 and using the following data: a) at room temperature the dichroic ratio $A_{\parallel}/A_{\perp}$ at the long-wavelength slope of the red LD band[1] reached 1.75, which for the ideal ordered system corresponded to ∠α = 78°; b) band 2 had the maximum anisotropy and was located between two bands with lower anisotropy (Table 1). Because of strong overlapping between these bands at room temperature, there was a significant decrease in the LD anisotropy of the sample recorded at band 2; c) incomplete ordering of sample also caused a decrease in the anisotropy value. Obviously, the angle of the dipole moment of the band 2 transition is significantly larger than 78° and the estimates of this angle are close to the limiting value.

The amplitude of the LhcIIb CD is ~0.4% absorption amplitude, which is typical of the spectra of exciton splitting and is three orders of magnitude larger than that value for pigments in solution.

Exciton (resonance) interaction emerges between two closely located identical chromophores. As a result, the individual specificity of the interacting chromophores is leveled and the spectral properties of the ensemble of chromophores are determined by its collective properties. An important property of exciton spectra is invariability of the mean values of $\Sigma E_i/n = E_0$; $\Sigma\mu_i^2/n = \mu_0^2$; $\Sigma C_i/n = C_0 \approx 0$, where subscripts *i* and 0 correspond to the exciton spectra and pigment monomers, respectively; *n* is the number of interacting molecules. Davydov's splitting [20] is another important manifestation of exciton interaction: absorption spectra instead of one band contain *n* characteristic narrow bands. The amplitudes of these bands in the fluorescence spectra are proportional to the population level and depend on temperature [20] in accordance with the Stepanov's equation (6). The most long-wavelength fluorescence band is dominant in low-temperature spectra. It follows from Fig. 1b that Eq. (6) is valid in the case of native LhcIIb.

The fact that the magnitude of splitting of the red band of Chl *b* lower than that of Chl *a* can be explained mainly by smaller dipole strength of Q_y transition in Chl *b*. It follows from Fig. 1c that in the blue spectral region at the Soret band exciton splitting is clearly seen in Chl *b* and the dipole strength of Chl *b* at the Soret band is higher than the dipole strength of Chl *a*. It follows from Fig. 3 and Table 1 that spectra of LhcIIb are superpositions of narrow alternating-sign CD and LD bands, which correspond to spectra of exciton splitting.

[1] Limiting value at α = 90° was 2.

Localization of chlorophylls in the LhcIIb subunit. Comparative analysis of spectral positions and dipole strength values in LhcIIb and chlorophyll monomer provides an opportunity to draw a borderline between the bands of Chl *a* (bands 1-7), bands of Chl *b* (bands 8-12), and satellite vibrational bands of Chl (bands 13-14) (Table 1).

Specific spectral features show that there are certain structures responsible for certain components of the Chl *b* absorption spectrum (Table 1): monomer (*B1*) demonstrating no anisotropy; dimer (*B2*) with alternating-sign CD and LD bands; and trimer (*B3*) with alternating-sign CD and LD bands, in which the third band is either weakly manifested (like a forbidden transition) or two bands with similar parameters merge together into one band (like a degenerate transition).

The number of bands, energy gaps between them, alternating-sign and conservative CD, the dipole strength values in the OD spectra nondivisible by μ_0^2, and presence of only one perpendicular transition in LD (band 7) suggest that the seven Chl *a* molecules produce one cluster (*A7*) with exciton interactions. The magnitude of the monomer term in CD is $C_0 = -0.088$ DM, which corresponds to the direction and rotation strength of Chl *a* in solution.

The chlorophyll clusters observed in these experiments are clearly seen in the crystallographic structure of the LhcIIb subunit [7]. There is a group of seven porphyrins in the stromal part of the subunit, another porphyrin molecule is located separately, and five molecules are in the lumenal part of the protein subunit (two molecules on one side and three molecules on the other side). Such topography of porphyrin molecules corresponds to four clusters of pigments (Table 1), the arrangement of which is shown in Fig. 4a.

The arrangement of porphyrins shown in Fig. 4a is consistent with a high efficiency of quenching of the triplet states of chlorophyll by *Car* molecules: four of seven Chl *a* molecules and three of five Chl *b* molecules are in contact with *Car* at the lumenal side of LhcIIb, whereas the triplets from the other molecules can migrate to *Car* by the exchange resonance mechanism through neighboring porphyrin molecules.

The isolated molecule *B1* is an exception. Therefore, the labile absorption band at 639.6 nm corresponds to the isolated position of this molecule. Localization of *B1* near the mobile N-terminal domain of the protein is supported by the results of treatment of the LhcIIb preparation with trypsin and chymotrypsin. This treatment causes degradation of the N-terminal domain of the protein [16] and disappearance of the band at 640 nm. The short-wavelength spectral position of this molecule and effective excitation migration to Chl *a* provide this molecule with high stability[1]. These bands are well resolved in chloroplasts of higher plants.

It should be noted that the wavelength of the spectral band of *B1* is shorter than that of Chl *b*. Therefore, *B1* differs chemically from common Chl *b*. In this case, chemical methods of measurement of concentration of pigments in LhcIIb may give erroneous estimates. This can explain an unexpectedly large ratio Chl *a*/Chl *b* (Chl *a*/Chl *b* = 1.47) observed for LhcIIb in [10, 11]. It seems fairly probable that *B1* is a product of oxidation of Chl *a* to a Chl *b*-like molecule. There is no such oxidation in *Chlorophyta*: the main light-harvesting complex LhcII in chlorella is characterized by the ratio Chl *a*/Chl *b* = ~1.6 and by the absence of the absorption band at ~640 nm. The shape of the absorption spectrum of this complex differs significantly from the LhcIIb absorption spectrum and resembles the spectrum of component 3 (Fig. 2). Perhaps, the eight porphyrin molecules at the stromal side of LhcIIb of green algae are Chl *a* molecules, whereas the five porphyrins at the lumenal side, are Chl *b* molecules.

Localization of pigments in Fig. 4a is characterized by a trend toward an ideal segregation[1], which is implemented in green algae: all Chl *a* molecules in green algae are at the stromal side, whereas the whole (standard) set of the Chl *b* molecules is exposed to the lumenal side of LhcIIb.

Configuration of chlorophyll *a* cluster in LhcIIb. The validity of the configuration of chlorophyll molecules shown in Fig. 4a is confirmed by the results of calculation of the geometry of the Chl *a* cluster from the exciton spectral parameters (Table 1): spectral parameters are determined by the geometry of the dipole moments of corresponding transitions (length and direction of the dipole moment of the transitions of monomers) (μ) and their mutual orientation, which can be characterized by the radius-vector (R) drawn from the geometrical center of the exciton cluster to the dipole center. On the polar frames of reference, directions of μ and R determine the values of two angles: $\angle\alpha$ with Z-axis (normal to the LhcIIb plane) and $\angle\varphi$ between the horizontal projection of the vector and X-axis. The length of μ is the same in all molecules ($\mu = 5.55$ D), whereas the length of R is the fifth parameter that determines the μ position in space.

The main energy operator (Hamiltonian **H**) in the steady-state approximation of the Schrödinger equation $\mathbf{H}\Psi = E\Psi$ is a symmetric matrix of 7×7 elements. The diagonal elements of the matrix are energies of monomer transitions and the other elements represent the energies of paired interactions. The eigenvalues of **H** are energies of exciton transitions E_i, which correspond to the eigenvectors $\Psi_i = \{a_{ki}\}$. Coefficients $\Psi^2 = \{a_{ki}^2\}$ represent the contribution of the *k*-th component to the *i*-th exciton

[1] The rate of interconversion (triplet formation) efficiency in chlorophyll molecules is ~1000 times smaller than the rate of energy migration from *B1* to Chl *a*.

[1] Chl *b* is synthesized from Chl *a*, which has been already incorporated in LhcIIb, and chlorophyll *b* synthetase is accessible only from the lumenal side of the complex due to membrane stacking.

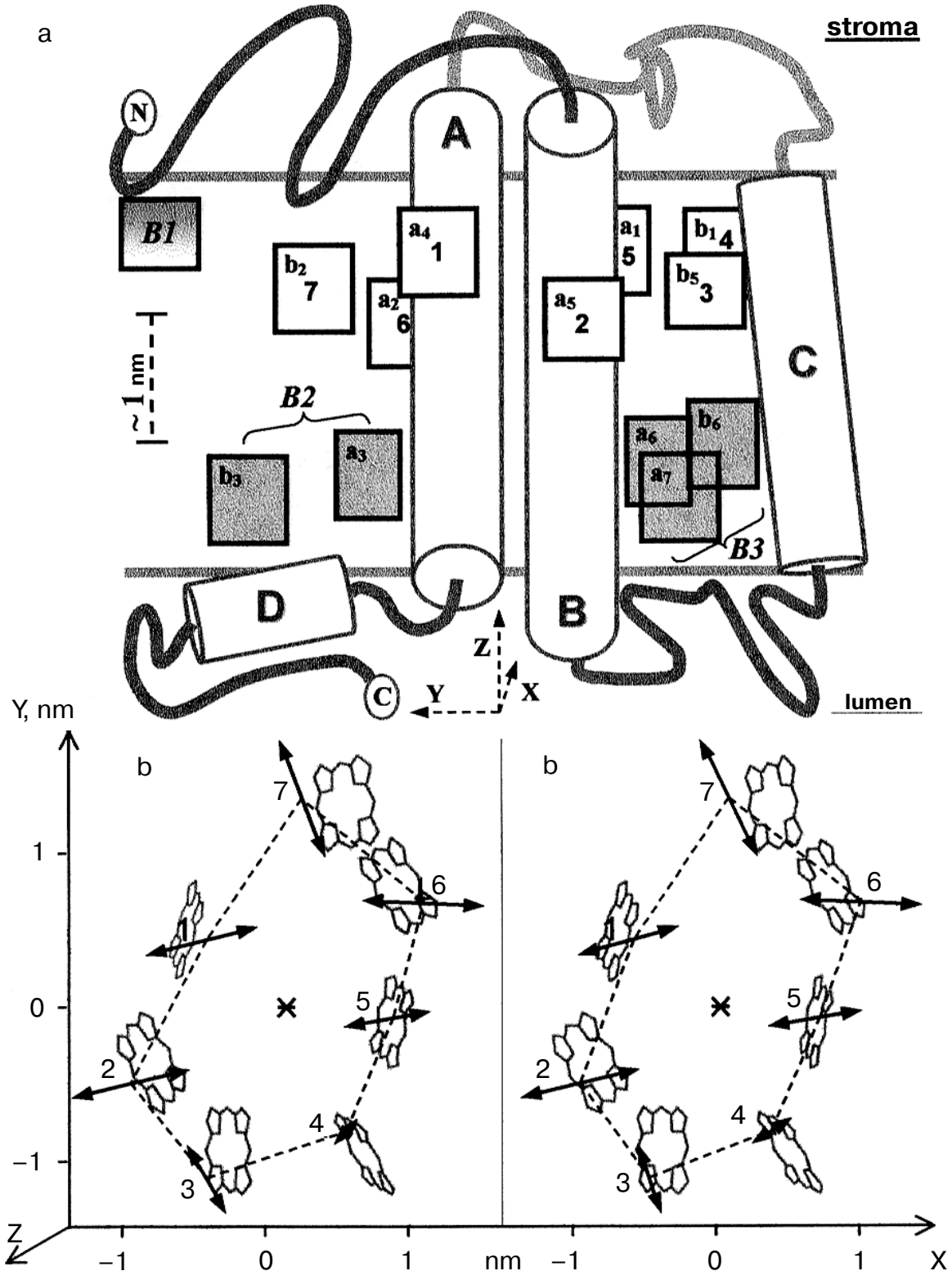

Fig. 4. Location of chlorophyll *a* molecules and clusters in the LhcIIb subunit. a) Membrane view from the trimer C_3-axis (direction C_3 coincides with vertical Z-axis). A, B, C, and D are protein α-helices. Porphyrins are denoted in accordance with the nomenclature accepted in this work and original nomenclature suggested by Kuhlbrandt et al. [6]. b) Stereoscopic diagrams of Chl *a* porphyrins and dipole moments of transitions of Chl *a* molecules in the LhcIIb subunit. The geometrical center of the dipoles (origin of coordinates) is indicated with an asterisk. Dipoles are drawn on a scale: 1 D = 1 Å. The centers of the dipoles of neighboring Chl *a* monomers are connected with segments. 1-7) Numbers of Chl *a* porphyrins; *B1*, *B2*, and *B3* are the Chl *b* monomer, dimer, and trimer, respectively.

transition and the probability of localization of the *i*-th excited level of exciton in the *k*-th monomer.

It was noted in the introductory part that there were grounds to believe that the LhcIIb spectrum was exclusively determined by specific features of exciton interactions within the LhcIIb subunit. Because the main absorption bands of Chl *a* and Chl *b* only insignificantly overlap with one another (Fig. 1a), the resonance interaction between these pigments could be regarded as negligible. Therefore, Chl *a* and Chl *b* in this case can be regarded as independent molecules. The area of partially symmetric oscillations of Chl *a* (~620 nm) can also be regarded as independent of the area of the main red bands of Chl *a* [20]. Therefore, parameters of the main Q_y bands obtained as a result of deconvolution of spectra (bands 1-7 of Chl *a* and bands 8-11 of Chl *b*, Table 1) were used as experimental data in model calculations. It is obvious that no calculations were performed for monomer *B1*.

The calculations were made by the simplex method with different initial values of dipole moment vectors. The energy and geometry parameters calculated using this approach are given in Table 2 (parameters of Chl *b* are given on internal coordinates). It follows from Table 2 that the distances between the closest neighbors in the Chl *a* ring are 8.4-11.7 Å and the energy of interaction between them[1] is 21-197 cm^{-1}. The distances between the closest neighbors in the Chl *b* ring are 7.4-13.4 Å and the values of the energy of interaction between them are 26 and 34 cm^{-1}.

The spectral parameters calculated based on the exciton models of clusters are given in Table 1. The spectra calculated from these data are shown in Fig. 3a. It follows from Fig. 3a that the three theoretically calculated spectra are a sufficiently close fit of experimental data. Both specific features and spectral structure are well pronounced, except the OD spectrum at the main maximum region. It should be noted that because the models were calculated based on parameters rather than spectra, the coincidence between experimentally measured and theoretically calculated spectral parameters was particularly important. It follows from Table 1 that there is a good correlation between the experimentally measured and theoretically calculated values.

Detailed analysis of correlation of the geometry of the Chl *b* clusters with crystallographic data is beyond the scope of this work. Because the trimer *B3* spectrum contains only two bands, its calculation is ambiguous. The structural model considered in this work was constructed assuming that the short-wavelength band at 649.8 nm was doubly degenerate (Table 2) and this model should be regarded as rather illustrative. The centers of the dipoles 4 and 5 are approximately in the plane XY, whereas the center of the dipole 3 makes a virtually vertical triangle with the centers of the dipoles 4 and 5. Mutual orientation of dipole moments of Chl *b* on the internal coordinates of the dimer and trimer is critical only to the LD value, i.e., to the spatial parameters along the Z-axis. Therefore, the structures can rotate freely about the Z-axis and turn upside down. In addition, the axis connecting the *B2* molecules is located close to the XY plane. Therefore, rotation around this axis is also allowed and position of *B2* in space is rather arbitrary. The distances between the Chl *b* molecules given in Table 2 are fairly realistic.

The spatial positions of vectors of dipole moments of the Chl *a* transitions are shown in the stereoscopic diagram shown in Fig. 4b. The dipoles produce a ring of an irregular shape. The dipoles are numerated in the anticlockwise direction.

Positions of porphyrin rings in Fig. 4b are given based on the results reported in [7]. It should be noted that the vector of the main dipole moment of the Q_y-transition in a chlorophyll molecule is directed along the porphyrin ring diagonal. Although the similarity between the Chl *a* dipole moment structures and similar location of seven porphyrins in the stromal part of LhcIIb are quite evident, they are far from ideal. The causes of incomplete correspondence are also fairly obvious: insufficient precision of the Kasha–Tinoco approximation used in calculations, errors in determination of band parameters, influence of Chl *b* and chlorophylls of neighboring subunits, and variability of transition energy of monomers (diagonal elements of Hamiltonian). These factors affect distribution of transition frequency and dipole strength values.

The most important specific properties of the LhcIIb subunit associated with protein structure are clearly manifested in the structure of dipole moments. In particular, nearly C_2-symmetry of the geometry of pairs of porphyrins and dipoles 1-5 and 2-6 corresponds to close to crystallographic position of centers of dipoles (Fig. 4b). Incomplete correspondence in this case may be partially caused by the conformational difference between the LhcIIb complexes used in this work and in crystallographic studies [7]. In other words, the spectra of the LhcIIb preparation used in the crystallographic studies differed from the spectrum shown in Fig. 3a. This suggestion is fairly realistic because the absorption spectra of the LhcIIb complexes may have features of minor difference though remaining similar to each other (see above).

Migration of excitation energy in the LhcIIb subunit. Excitons are generated in molecular ensembles as a result of exciton (resonance) interaction between several dipole moments of transitions with one photon. The phenomenological properties of the Chl *a* excitons in LhcIIb are similar to the phenomenological properties of excitons with strong interaction (energy of paired interaction is

[1] The energy sign in paired interactions is arbitrary: the lengths of μ in the opposite directions may be equal to one another. The change in the direction of a vector changes the sign of the energy of paired interaction to the opposite one.

Table 2. Parameters of exciton interaction between molecules in the LhcIIb subunit. α is the angle with Z-axis (normal to trimer plane); φ is the angle of the plane projection with X-axis. The numbers of the Chl *a* molecules correspond to those in Fig. 4. The numbers of the exciton transitions (*1-7* and *8-11*) correspond to those in Table 1. Spectra are shown in Fig. 3a

		Parameters of transitions of Chl *a* molecules						
	No.	1	2	3	4	5	6	7
$\bar{\mu}$	α (°)	61.6	87.5	48.6	37.9	68.1	91.7	58.3
	φ (°)	15.4	−152	−64	−115	−153	13.2	142
$\bar{R}$	α (°)	69.1	123	108	71.9	71.1	96.6	76.4
	φ (°)	167	−149	−101	−55	2.8	50.6	104
	R, Å	7.6	11.5	11.3	10.0	7.3	12.2	12.5
		Hamiltonian (energy of paired interaction), cm^{-1}						
Distance, Å	1	14916	−21	29	−9	76	−37	−70
	2	11.2	14916	197	36	−17	21	26
	3	14.5	8.8	14916	80	8	13	9
	4	15.5	16.9	10.4	14916	−117	11	20
	5	13.9	18.2	15.3	8.4	14916	−61	−3
	6	17.1	22.0	22.3	17.9	9.8	14916	171
	7	11.0	19.9	23.3	21.3	15.1	11.7	14916
		Parameters of exciton transitions of Chl *a* molecules						
	No.	*7*	*6*	*5*	*4*	*3*	*2*	*1*
	α (°)	32.5	117	58.8	56.7	60	88.4	73.8
	φ (°)	−116	75.9	157	13.5	−161	149	22

	cluster	*B2*		*B3*		
		Parameters of transitions of Chl *b* molecules				
	No.	1	2	3	4	5
$\bar{\mu}$	α (°)	96.7	45.6	50.5	108	42.5
	φ (°)	116	45.6	11.8	99.4	25.4
$\bar{R}$	α (°)	96.2	83.8	45.5	104	122
	φ (°)	0	180	−124	30.3	180
	R, Å	6.7	6.7	5.9	7.1	4.3
		Hamiltonians, cm^{-1}				
Distance, Å	1	15473	26			
	2	13.4	15473			
	3			15356	−34	−34
	4			12.3	15356	−34
	5			7.4	10.2	15356
		Parameters of exciton transitions of Chl *b* molecules				
	No.	*11*	*10*	*9′*	*9*	*8*
	α (°)	67.5	129	127	132	59.9
	φ (°)	87.4	158	−42.8	140	48.8

Table 3. Time of radiationless transition of the excitation energy between the LhcIIb pigment clusters and between components of *M*PSII at 77 K, psec (10^{-12} sec). Tabular values of time t_T are given for R = 3 nm and $k = 1$; $t(R,k) = t_T (R/3)^6/k^2$; R is the distance (nm); k is the orientation factor*. The time values in *M*PSII are given for the components normalized to seven Chl *a* molecules. *B2*, *B3* are the dimer and trimer of the Chl *b* molecules, respectively; *A7* is the heptamer of the Chl *a* molecules

		Acceptor					
		B3	*A7*		**LhcIIb**	**CON**	**PSII core**
Donor	*B2*	23	25	**LhcIIb**	25	21	17
	B3	—	8	**CON**	39	27	19
	A7	—	16	**PSII core**	187	111	66
	LhcIIb			***M*PSII**			

* $0 \le k^2 \le 4$; the three-dimensional mean $k^2 = 2/3$; mean value in a plane, $k^2 = 5/4$.

~100 cm^{-1}, see Table 2) and are represented by a collective excited state of the molecules, in which the excitation with lifetime 10^{-13} sec is delocalized over the molecules [20, 24]. In the quantum processes these excitons are equivalent to the excited state of one molecule with a complicated multilevel spectrum and the maximum density of excitation near the geometrical center of the exciton cluster.

The exciton transition from one level to another occurs during vibrational relaxation within the time interval 10^{-13} sec [20]. This time interval is sufficient to attain the state of thermal equilibrium between the levels [20]. The magnitudes and phases (directions) of the contributions of monomers to the excited state are changed during the transition between the levels (so-called dephasing) [24]. It was found experimentally that the dephasing time in LhcIIb at 77 K within the spectral range 660-679 nm was indeed equal to ~10^{-13} sec [13].

Even in the state of thermal equilibrium, the process of exciton migration occurs by the mechanism of slow inductive resonance (Eq. (5)). The efficiency of this type of energy migration significantly depends on the overlapping between the fluorescence spectrum of the excitation donor and the absorption spectrum of the excitation acceptor. The values of the time of the excitation migration between the LhcIIb chlorophyll clusters and between components of *M*PSII were calculated from Eq. (5). The results of these calculations are given in Table 3. It follows from the laws of thermodynamics that the time of excitation transition is inversely proportional to the dipole strength of the excitation acceptor absorption (number of Chl *a* molecules).

The distance between the centers of clusters in the subunit is ~20 Å. The values of the time of the excitation migration in the systems *B1*→*A7*, *B2*→*A7*, and *B2*→*B3* are thought to be about several picoseconds. The long-wavelength transition (No. 8) is dominant in the fluorescence spectrum of cluster *B3*. There is the maximum overlap between the spectrum of this transition and spectrum of transition No. 6 in cluster *A7*. The slope angles of these spectra are close to one another (30 and 28°, respectively, Table 1). In this case the value of the orientation factor k^2 for the pair *B3*→*A7* may approach the maximum level (~4), whereas the time of the excitation transition *B3*→*A7* is ~$2 \cdot 10^{-13}$ sec, or ~0.2 psec. Such lifetimes in the picosecond and subpicosecond[1] time ranges were observed in studies of relaxation of the Chl *b* excited state in LhcIIb [10, 11, 13, 14, 28].

Spectra of LhcIIb and *Car* within the absorption range of *Car* and Soret band of chlorophylls are shown in Fig. 1c. It follows from Fig. 1c that the fluorescence excitation spectrum of the sample virtually coincides with the OD spectrum. Therefore, the whole amount of the excitation energy of *Car* effectively migrates to Chl *a*. However, the probability of direct excitation from the low-energy level of *Car* to Chl *a* is low, because the absorption of Chl *a* near 500 nm is negligible and any resonance (inductive resonance or exchange resonance) processes are unrealistic. This conclusion is supported by the following findings: a) effective migration in core-complex PSI, where the most long-wavelength band of carotene at ~520 nm overlaps with the Q_x band of chlorophyll *a* (~590 nm with a satellite at ~540 nm); b) low efficiency of migration from carotene to Chl *a* in PSII, where spectral positions of β-carotene and *Car* are close to one another.

It follows from Fig. 1c that the long-wavelength band of *Car* and Soret band of Chl *b* in LhcIIb (at ~493 and

[1] The Förster equation is invalid at such short times. Therefore, the value of 0.2 psec should be regarded as a qualitative estimate: $t < 1$ psec.

~484 nm, respectively) significantly overlap with each other. This provides high efficiency of excitation energy transfer from *Car* to Chl *b* (and further to Chl *a*) in case of close location of these pigments in LhcIIb. This was the sequence of energy migration processes *Car*→Chl *b*→Chl *a* that was directly demonstrated using laser absorption spectroscopy [28].

Excitation energy migration between LhcIIb subunits. The processes of excitation energy transfer in LhcIIb are possible between the *A7* clusters of neighboring subunits, the distance between the centers of which is ~30 Å. The results of calculation of the cluster *A7* geometry and the third order axial symmetry of the LhcIIb trimer provide sufficiently accurate estimates of k^2 = 2.6-2.7 in Eq. (5). This also allows the time of the excitation energy migration between LhcIIb subunits to be determined (at R = 30 Å = 3 nm this time is 6 psec (Table 3)).

The following data can be used as experimental estimates of the migration time: a) dephasing in the long-wavelength absorption band of LhcIIb (~680 nm) at 4.2 K [15], because the anti-Stokes processes at this temperature are energy-forbidden and higher energy levels of exciton are not involved in the relaxation processes. This dephasing occurs within 10 psec and is probably accompanied by excitation transfer between the subunits; b) depolarization of excitation in LhcIIb, the time of which at 300 K is 5 psec [14]. This process can be also associated with the energy migration between the LhcIIb trimer subunits. The two estimates of the exciton migration time between the LhcIIb subunits give a value close to that calculated above (6 psec).

The mean distance between the closest LhcIIb *A7* clusters of neighboring LhcIIb trimer subunits in the *M*PSII particle (Fig. 5) is ~60 Å = 6 nm and the value of k^2 is 1.5-2.5. The time of the excitation migration between these clusters is $16 \times (6/3)^6/k^2$ psec (see Table 3) = 410-680 psec. The excitation in this case with the probability = 1/3 is localized in the subunit which is not in contact with neighboring subunits. As a result, the time of migration between the trimers is 3/2 times longer (i.e., ~600-1000 psec). This time is comparable with the time of excitation dissipation in LhcIIb and is much longer than the other characteristic times of excitation transfer. Obviously, the efficiency of the processes of the excitation migration between neighboring LhcIIb trimers in the photosynthetic membrane can be regarded as negligible.

The distance between the LhcIIb *A7* clusters of neighboring stacked membranes is ~35 Å (Fig. 4a) and the value of *k* is ~1. The time of the excitation migration between these clusters is ~40 psec. This time is shorter than the excitation lifetime in *M*PSII, thereby providing high efficiency of energy migration between stacked membranes.

The succession, characteristic times of energy migration, and calculated parameters of the Chl *a* molecular ensemble agree well with the pattern of arrangement of pigments in the LhcIIb subunit shown in Fig. 4a.

Structure of granal macrocomplex of PSII. In the granal regions of chloroplasts at the areas of PSII location the acceptor (stromal) surfaces of neighboring membranes densely stack to each other. The membrane stacking gives rise to the formation of the granal multicentral macrocomplex of PSII (*M*PSII), which is composed of two PSII particles of neighboring membranes (Fig. 5). Perhaps both LhcIIb and allied CON proteins play an important role in membrane stacking: the N-terminal stromal domains of these proteins are macrodipoles[1], the initial segment of which includes 4-9 cations and the next segment includes about the same number of anions [8]. The electrostatic interaction between these dipoles provides close contact between stacked membranes.

Photosystem 2 consists of RC, proteins CP43 and CP47 [21, 29] and incorporates ~36 porphyrin molecules [21, 22, 30]. Reaction center of PSII consists of two proteins and incorporates eight porphyrin molecules [29, 30]. In the photosynthetic membrane, PSII exists as a dimer [29, 31]. The deconvolution of the CON-protein absorption spectrum (Fig. 3b, curve *3*) into individual bands revealed that the CON-proteins were characterized by the mean[2] value of the Chl *a*/Chl *b* ratio equal to 2.6-2.7 = 8 : 3. Substantial similarity between the proteins of the LhcII family suggests that the subunit of the CON-protein incorporates about the same number of chlorophyll molecules and its size is approximately equal to the size of the LhcIIb subunit. According to the pigment ratio, the CON-proteins contain an average of eight Chl *a* and three Chl *b* molecules.

The *M*PSII absorption spectrum (Fig. 3b) corresponds to the following molar ratio: 36 Chl *a* molecules (21%) of core-complex monomer, 25 Chl *a* molecules (15%) of CON-proteins (three proteins), and 108 Chl *a* molecules (64%) of LhcIIb (five trimers). The *M*PSII particle in this particular example contained ten LhcIIb trimers associated with six CON-proteins bound to a core-complex dimer.

The structure of the core-complex dimer was resolved in [30] with resolution 3.8 Å. The shape and the surface relief of the *M*PSII particle containing a core-complex dimer, CON-proteins, and two LhcIIb trimers were determined in [31] with resolution ~2 nm. The second order axial symmetry was found to be inherent in all these structures. The model of the *M*PSII structure shown in Fig. 5 was suggested on the basis of generalization of the data considered above: a bent parallelogram of the *M*PSII particles described in [31] was inscribed in the core-complex dimer described in [30] taking into account the size and

[1] Amino acid residues of arginine (+), lysine (+), glutamic acid (−), and aspartic acid (−) [8].

[2] The presently available data do not allow three CON-proteins (CP29, CP26, and CP24) to be differentiated from one another [9]. Therefore, mean characteristics of CON-protein are used in this work.

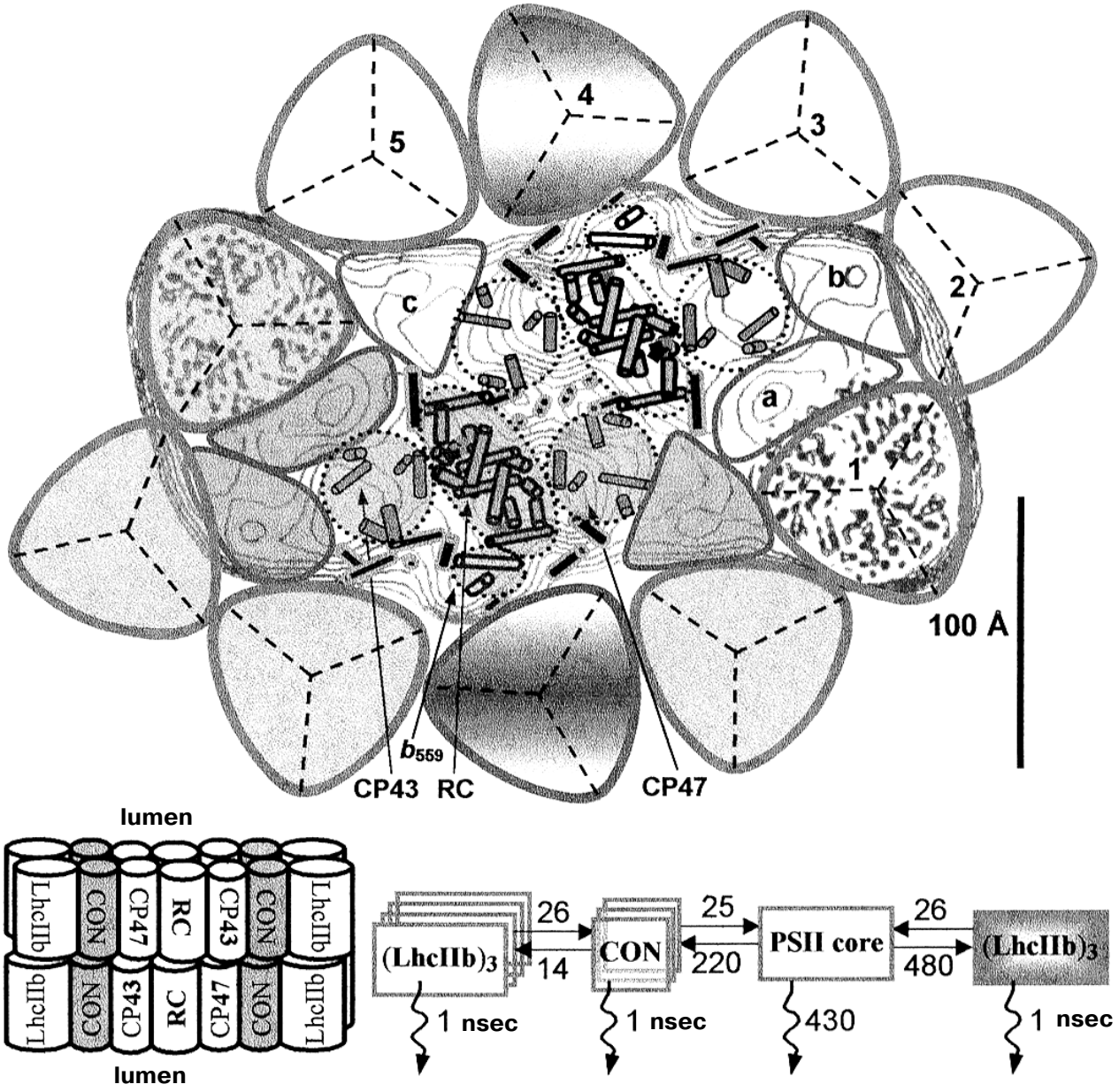

Fig. 5. Scheme of structural–functional organization of granal macrocomplexes of PSII. Scheme of the *M*PSII particle structure is shown at the top (view from the lumenal side). The central part of the particle is occupied by a dimer of the PSII core-complex. The proteins of the complex are circumscribed with ellipses. Cylinders show the α-helical domains of the proteins; a, b, c) CON-proteins (internal light-harvesting complexes CP24, CP26, and CP29); 1-5) LhcIIb trimers. Bottom: block diagram of *M*PSII and kinetic scheme with characteristic times at 77 K (psec) in *M*PSII with closed reaction centers; waved arrows show excitation dissipation; straight arrows show excitation energy migration accounted for relative concentration of chlorophyll in complexes.

relief of the particle. Core-complex proteins were denoted and positioned in accordance with [30]. The space between LhcIIb and core-complexes is filled with the units (a, b, c) of the size of the LhcIIb monomer and similar shape (exactly six such units are aligned). Additional LhcIIb trimers (Nos. 2-5) are placed along the perimeter observing the second order symmetry (exactly eight). The model shown in Fig. 5 is consistent with the stoichiometry of the *M*PSII preparation studied in this work. It is perhaps the largest possible *M*PSII structure. This particle contains 530 chlorophyll molecules per RC PSII dimer with the ratio Chl *a*/Chl *b* = 1.67. This value coincides with the value of the ratio Chl *a*/Chl *b* = 1.70 ± 0.05 experimentally measured in this preparation of *M*PSII.

In the chloroplast grana and in the isolated state two PSII particles stick together giving rise to a transmem-

brane tetramer [31]. The structure of the *M*PSII particle (Fig. 5) suggests the following scheme of the excitation energy migration: excitation from the LhcIIb trimers 1, 2, 3, and 5 is transferred to core-complex via CON-proteins, whereas from the LhcIIb trimer 4 it is transferred directly to core-complex.

Migration of excitation energy in the granal macrocomplex of PSII. There are features of remarkable similarity between the spectral characteristics of all PPC species producing the *M*PSII (Fig. 3b). Structural homology between the members of the family of the LhcIIb proteins [8] and similarity between their spectra in the OD range of Chl *a* (Figs. 2 and 4b) suggest that Chl *a* of CON-proteins produce a LhcIIb-like cluster near the stromal surface. The PSII absorption spectra at 77 K [21] are mainly due to the antenna proteins CP43 and CP47, whereas the RC PSII spectra show that Chl *a* in these complexes is arranged as exciton clusters [1, 21]. Thus, the excitation migration in *M*PSII should be calculated from Eq. (5) as suggested above for excitation migration between LhcIIb subunits.

The values of the excitation transfer time calculated for equal concentrations of Chl *a* (normalized to seven molecules of LhcIIb) are given in Table 3. The spectra of *M*PSII and its components (core-complex, LhcIIb, and CON-protein) shown in Fig. 3b provide an opportunity to calculate the values of the rate (time) of the excitation energy migration between the main compartments of *M*PSII.

Because of the symmetry of the system, the excitation dynamics in *M*PSII is characterized by four states with different localization of excitation: 1) at LhcIIb (Nos. 1, 2, 3, and 5); 2) at CON-protein; 3) at core-complex; 4) at LhcIIb (No. 4). Excitation transport between identical components is not represented kinetically.

The resulting kinetic scheme of *M*PSII is shown in Fig. 5 together with the times of the excitation migration at 77 K, which were calculated taking into account the pigment stoichiometry in the complexes. The spectra of an aggregated preparation of LhcIIb were used in these calculations. This preparation was characterized by low amplitude of the F spectrum at 700 nm (Fig. 3b) and fluorescence lifetime 1 ± 0.1 nsec. This value of the fluorescence lifetime was taken to be equal to the time of excitation relaxation in the two types of LhcII, whereas its error ($\pm 10\%$) is characteristic of the error of the time calculation in the scheme shown in Fig. 5.

The calculated time of the excitation relaxation in core-complex (430 ± 43 psec) coincides with the time determined earlier in the PSII of the cyanobacteria *Synechocystis* sp. and *A. nidulans* (~460 psec) [22]. It should be noted that this value is the mean integral time of excitation relaxation in PSII with closed RC (state F_m) including the time of excitation migration within the core-complex, time of exciton decay (charge separation) in RC, recombination time of separated charges in RC, and time of migration of recombinant exciton in core-complex.

One of the three LhcIIb subunits shown in the structural scheme (the probability of the excitation localization in the subunit is 1/3) neighbors with an average of 1.5 CON-proteins containing $8 \times 1.5 = 12$ Chl *a* molecules. The time of excitation transfer from the cluster *A7* of the subunit to CON-proteins is one-third of 26 psec = ~9 psec (Fig. 5). The time $t = f(R, k^2, [\text{Chl } a \text{ acceptor}]) = t_T \times (R/3)^6/k^2 \times 7/12$ allows the mean distance (t_T = 21 psec, Table 3) to be calculated. The excitation in LhcIIb is actually transferred between the long-wavelength transitions. All these transitions in LhcIIb are polarized in the plane close to the LhcIIb trimer plane. Therefore, the averaged variant of migration considered in this work corresponds to $k^2 = 1.25$ and $R = 2.94$ nm. The resulting mean distance between the centers of the exciton clusters of CON-proteins and closest LhcIIb subunit agrees well with the structure shown in Fig. 5.

Both this distance and the time of migration virtually coincide with the estimates obtained for the subunit in the LhcIIb trimer. Actually, the LhcIIb–CON-protein complexes can be regarded as tetramers. The results of electrophoresis show that such tetramers indeed exist (Fig. 2).

The kinetics of energy migration is described by the first-order equations. The time values used in this work to characterize the rate of migration are reverse rate constants. In other words, characteristic time of energy migration is inversely proportional to the density of the probability of the excitation hopping between the components. This raises the problem of the physical sense of the characteristic times (e.g., 26-psec migration from LhcIIb to CON-proteins and 14-psec migration in the reverse direction) (Fig. 5). These values mean that the concentration of excited states in LhcIIb either exponentially decreases in accordance with the following equation $C_1 \times \exp(-t/26)$ or exponentially increases in accordance with the following equation $C_2[1 - \exp(-t/14)]$ (t is time, psec), if these processes are unique and independent. But the interaction between these processes would give rise to the situation in which none of the characteristic times shown in Fig. 5 is manifested individually. Therefore, experimental measurement of these characteristic times in this situation is impossible in principle.

Absorption of a light quantum induces formation of an exciton in small clusters of antenna pigments. The properties of the clusters are determined by their structure (interaction between pigments). The thermal equilibrium of the excitation energy distribution between the exciton energy levels is attained within ~0.1 psec. Within the protein subunit, the thermal equilibrium is attained within ~1 psec. Both in LhcIIb and in CON-proteins excitation is concentrated in the stromal regions of the complexes, where Chl *a* clusters are localized and exciton migration from *M*PSII occurs mainly near the stromal surface of the membrane. Exciton transfer between the Chl *a* clusters of neighboring proteins occurs within ~10 psec.

The number of LhcIIb per chloroplast *M*PSII may vary. Usually, the oxygen-evolving preparations of *M*PSII are characterized by the chlorophyll *a/b* ratio Chl *a*/Chl *b* = ~2. This value corresponds to three LhcIIb trimers per RC PSII. In other words, the peripheral ellipse of the LhcIIb trimers shown in Fig. 5 should be broken, because there are only six of ten trimers. Perhaps, the trimers 2 and 4 are absent. Both the scheme and characteristic time values shown in Fig. 5 should be subjected to rather obvious correction to fit the structure of this *M*PSII.

If the long-wavelength bands and excitation quenching in LhcIIb are absent, the time of relaxation in LhcIIb increases from 1 to ~2 nsec (as in the LhcIIb trimer). In contrast to that, the time of migration from LhcIIb to CON-proteins and to core-complex in this case decreases from 26 to ~20 psec. The changes in the two parameters cause an increase in the quantum yield of the photochemical reactions in *M*PSII.

At physiological temperatures the thermal equilibrium energy values of excited states of all PPC in *M*PSII fall within a narrow range (ΔE = ~70 cm^{-1} << $kT \approx$ 210 cm^{-1}). Therefore, energy migration in this case is virtually equidirectional and probability of localization of excitation at any *M*PSII site is proportional to the Chl *a* concentration at the site. This property provides high efficiency of the processes of back transfer of excitation from closed or functionally inactive RC to open RC.

High velocity of exciton movement between Chl *a* clusters near the stromal surface of the photosynthetic membrane is able to compensate the lack of directional energy migration and places substantial limitation on the number of elementary acts of energy migration in antenna preceding excitation trapping in RC. Cooperative functioning of four RC in *M*PSII provides necessary efficiency of energy transformation and trapping.

Preparative electrophoresis was performed by my late colleague, Prince V. M. Golitsin (April 19, 1951-October 21, 2000). We will always retain a kind and loving memory of this wonderful person.

REFERENCES

1. Tetenkin, V. L., Gulyaev, B. A., Seibert, M., and Rubin, A. B. (1989) *FEBS Lett.*, **250**, 459-463.
2. Gulyaev, B. A., Tetenkin, V. L., and Pomerantseva, O. M. (1979) *Dokl. Akad. Nauk SSSR*, **248**, 752-756.
3. Gulyaev, B. A., and Tetenkin, V. L. (1980) *Dokl. Akad. Nauk SSSR*, **250**, 1251-1255.
4. Gulyaev, B. A., and Tetenkin, V. L. (1981) *Biofizika*, **26**, 288-294.
5. Tetenkin, V. L., Golitsin, V. M., and Gulyaev, B. A. (1997) in *Problems and Trends of Photobiochemistry*, Moscow, p. 77.
6. Kuhlbrandt, W., and Wang, D. N. (1991) *Nature*, **350**, 130-134.
7. Kuhlbrandt, W., Wang, D. N., and Fujioshi, Y. (1994) *Nature*, **367**, 614-621.
8. Jansson, S. (1994) *Biochim. Biophys. Acta*, **1184**, 1-19.
9. Peter, G. F., and Thornber, J. P. (1991) *J. Biol. Chem.*, **266**, 16745-16754.
10. Hemelrijk, P. W., Kwa, S. L. S., van Grondelle, R., and Dekker, J. P. (1992) *Biochim. Biophys. Acta*, **1098**, 159-166.
11. Kwa, S. L. S., Groeneveld, F. G., Dekker, J. P., van Grondelle, R., van Amerongen, H., and Struve, W. S. (1992) *Biochim. Biophys. Acta*, **1101**, 143-146.
12. Van Amerongen, H., Kwa, S. L. S., van Bolhuis, B. M., and van Grondelle, R. (1994) *Biophys. J.*, **67**, 837-847.
13. Schubert, A., Voigt, B., Leupold, D., Beenken, W., Ehlert, J., Hoffman, P., and Lokstein, H. (1997) *Biochim. Biophys. Acta*, **1321**, 195-199.
14. Savikhin, S., van Amerongen, H., Kwa, S. L. S., van Grondelle, R., and Struve, W. S. (1994) *Biophys. J.*, **66**, 1597-1603.
15. Reddy, N. R. S., van Amerongen, H., Kwa, S. L. S., van Grondelle, R., and Small, G. J. (1994) *J. Phys. Chem.*, **98**, 4729-4735.
16. Nussberger, S., Dekker, J. P., Kuhlbrandt, W., van Bolhuis, B. M., van Grondelle, R., and van Amerongen, H. (1994) *Biochemistry*, **33**, 14775-14783.
17. Van Amerongen, H., van Bolhuis, B. M., Betts, S., Mei, R., van Grondelle, R., Yocum, C. F., and Dekker, J. P. (1994) *Biochim. Biophys. Acta*, **1188**, 227-234.
18. Nakayama, K., and Mimuro, M. (1994) *Biochim. Biophys. Acta*, **1184**, 103-110.
19. Kehrberg, G., Voight, J., Schrotter, T., and Renger, G. (1995) *Biochim. Biophys. Acta*, **1231**, 147-156.
20. Davydov, A. S. (1968) *The Theory of Molecular Excitons* [in Russian], Nauka, Moscow.
21. Gulyaev, B. A., Golitsin, V. M., and Tetenkin, V. L. (1988) *Dokl. Akad. Nauk SSSR*, **301**, 993-997.
22. Tetenkin, V. L., Golitsin, V. M., and Gulyaev, B. A. (1998) *Biochemistry (Moscow)*, **63**, 584-591.
23. Vernon, L. P. (1960) *Analyt. Chem.*, **32**, 1144-1160.
24. Pearlstein, R. M. (1982) in *Photosynthesis: Energy Conversion by Plants and Bacteria* (Govinjee, ed.) Academic Press, New York, p. 293.
25. Neporent, B. S. (1970) in *Molecular Photonics* [in Russian], Nauka, Leningrad, p. 18.
26. Stepanov, B. I. (1972) *Zh. Prikl. Spektr.*, **17**, 245-251.
27. Kasha, M., Rawls, H. R., and El-Bayoumi, M. A. (1975) *Pure Appl. Chem.*, **11**, 371-392.
28. Connelly, J. P., Muller, M. G., Bassi, R., Croce R., and Holzwarth, A. R. (1997) *Biochemistry*, **36**, 281-287.
29. Seibert, M. (1995) *Aust. J. Plant Physiol.*, **22**, 161-166.
30. Athina Zouni, A., Witt, H.-T., Kern, J., Fromme, P., Kraus, N., Saenger, W., and Orth, P. (2001) *Nature*, **409**, 739-743.
31. Boekema, E. J., Hankamer, B., Bald, D., Kruip, J., Nield, J., Boonstra, A. F., Barber, J., and Rogner, M. (1995) *Proc. Natl. Acad. Sci. USA*, **92**, 175-179.